J. Fluid Mech. (1973), *vol.* 61, *part* 3, *pp.* 481–498
Printed in Great Britain

Nearly spherical constant-power detonation waves as driven by focused radiation

By Y. H. GEORGE† AND F. K. MOORE
Sibley School of Mechanical and Aerospace Engineering,
Cornell University, Ithaca, New York

(Received 19 April 1973)

An analysis is made of the flow within a three-dimensional explosion, or spark, created in a gas absorbing energy from a steady conical beam of radiation with nearly spherical symmetry. The radiation, typically from an array of lasers with a common focus, is assumed to be very intense, and absorbed immediately behind an outwardly advancing strong shock. The resulting self-similar flow has previously been studied for spherical symmetry; somewhat improved calculations for that case are presented here.

Departures of the laser power from spherical uniformity, which would result from practical problems of arrangement, are conveniently represented by an ascending series of Legendre polynomials in the polar angle. For non-uniformities of small amplitude, first-order perturbations of the flow field are analysed in detail. Self-similarity is shown to be retained, for zero counter-pressure and power constant with time.

For the first five harmonics in power distortion, the resulting fourth-order system of equations is solved numerically for profiles of velocity components, density and pressure, and for shock shape. Results are presented graphically. These solutions are singular near the focus, but are nevertheless fully determined. In the limit of large wavenumber, the core of the flow has vanishing tangential velocity and pressure perturbations, and hence the governing equations are only of second order, except presumably in a boundary layer appearing near the shock.

Study of the nonlinear case of large wavenumber along the axis of symmetry shows that the singularity at the focus reflects the existence of a 'forbidden zone' whose extent depends on the degree of asymmetry. It is argued that this zone is one within which diffusional processes must dominate.

1. Introduction

Recent efforts in the field of nuclear fusion together with the development of very powerful pulsed lasers underline the importance of laser breakdown of matter. Early research in this field, by Meyerand & Haught (1963) and by Damon & Tomlinson (1963), concerned the breakdown of gases to create plasma explosions. Experimental evidence is abundant (see the review of Demichelis 1969) and deals with three distinct phases of the phenomenon: initiation of breakdown, growth of the plasma during the laser pulse and finally, decay of the plasma

† Present address: Ateliers de Construction Electrique de Charleroi, Charleroi, Belgium.

after termination of the pulse. The initial breakdown in a gas seems to occur by multi-photon ionization followed by cascade ionization. The final decay of the spark after the pulse has been explained by Panarella & Savic (1968) in terms of non-spherical blast-wave theory under the 'locally radial' approximation.

As for the intermediate phase, the interaction of laser radiation with the developing plasma, three mechanisms have been suggested, all essentially one-dimensional. The 'radiation-supported detonation wave' was proposed by Ramsden & Savic (1964) and later improved by Raizer (1965), Daiber & Thompson (1967) and Key (1969). Several 'breakdown wave' mechanisms, based on various breakdown criteria, were proposed by Raizer (1965), Ambartsumyan *et al.* (1965), Canto, Reuss & Veyrie (1968) and Alcock *et al.* (1968). Finally, a 'radiation transport wave' was also discussed by Raizer (1965). The appropriate theoretical model seems to be determined by the physical nature of the plasma and the time history of the laser pulse.

Although most experiments reported to date have relied upon a singly focused laser resulting in very oblong sparks, it is clear that a spherical arrangement using a battery of lasers will increase the energy input into the plasma. Indeed, quite a few experiments are now in progress using optical systems which split an original beam and redirect each component in a different direction; up to 27 beams will, it is hoped, be generated and focused in this way. The fluid-mechanical consequences of such a nearly spherical focused power deposition constitute the subject of this paper.

The theory of spherical sparks has been independently developed by Champetier, Couairon & Vandenboomgaerde (1968) and Wilson & Turcotte (1970). Both groups made use of self-similarity in the case of constant power addition, and numerically integrated the flow equations in a velocity–temperature plane. They found that the wave front is an overdriven detonation wave (subsonic conditions behind the front).

In the present paper, such a spherically uniform power addition is slightly distorted as a function of the polar angle. The resulting theory applies directly only to experiments with several coaxial conical beams with a common focus, but slightly different intensities. The laser radiation is assumed to be completely absorbed in a narrow layer following the leading shock wave; the plasma is considered to be a perfect gas with zero viscosity and heat conduction, and thermal reradiation is neglected in comparison with the laser power input. Self-similarity of the flow within the shock envelope is obtained if the pressure ahead of the shock is negligible compared with that behind, and if the power does not vary with time. For laser-generated explosions of solid targets, the plasma expands into a vacuum; thus, the physical concepts are the same during the plasma–laser radiation interaction phase and the present analysis is applicable to that case also. It may be remarked that the Newtonian approximation $\gamma = 1$ is not useful for the case of power constant in time, in contrast to the blast wave of constant energy.

Given the power perturbation, we obtain the shape of the spark, and the conditions just behind the front are derived. The inner flow is expressed as a Fourier series, and radial profiles of all physical variables are given for harmonics 1–4.

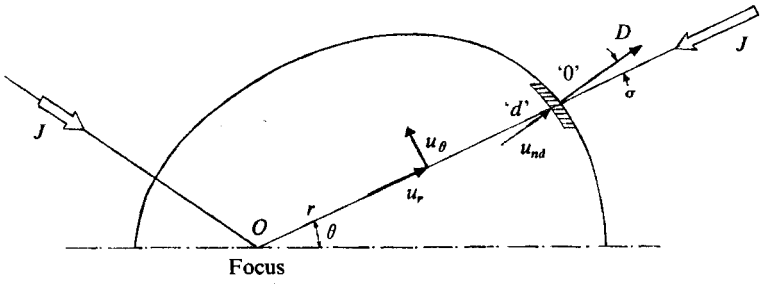

FIGURE 1. Geometrical arrangement of a laser-induced spark.

The analysis brings out the existence of a focal singularity, namely the presence of a 'forbidden region' near the origin. This rather surprising result seems to be connected with the geometry of the perturbation. It is suggested that this singularity could probably be removed by introduction of diffusion to smooth out the very strong angular gradients which otherwise exist near the origin.

2. Governing equations

In this section, hydrodynamic equations and boundary conditions are presented for a general geometry. Figure 1 shows the laser heat flux J converging to a focus O, with cylindrical symmetry about the horizontal axis. The wave front comprises a curved shock wave followed immediately by a region in which the energy carried by the laser photons is absorbed. Conditions in the undisturbed medium are marked '0' and conditions just behind the absorption layer are marked 'd'. Also, D is the normal component of the wave-front velocity and u_{nd} is the gas velocity behind the front; σ is the angle between D and J.

Assuming a narrow absorption layer (such as in air at normal density and very high temperature) and neglecting radiation pressure and energy, we obtain from conservation of mass, momentum and energy a set of boundary conditions to be applied at d:

$$u_{nd} = D(1-f), \quad \rho_d = \rho_0/f, \tag{2.1a,b}$$

$$p_d = p_0 + \rho_0 D^2(1-f), \tag{2.1c}$$

$$f = \frac{1}{\gamma+1}\left\{\gamma + \frac{1}{M_D^2} \pm \left[\left(1-\frac{1}{M_D^2}\right)^2 - 2(\gamma^2-1)\frac{J\cos\sigma}{\rho_0 D^3}\right]^{\frac{1}{2}}\right\}. \tag{2.1d}$$

ρ is the density, p is pressure, γ is the ratio of specific heats at constant pressure and volume, and M_D is the front Mach number based on the velocity D and sound speed in the undisturbed medium. It may be noted that the present energy-exchange model implies a 'radiation parameter' $(\gamma^2-1)J\cos\sigma/\rho_0 D^3$ of order unity, driving the shock. The plus sign in (2.1d) corresponds to an underdriven wave which degenerates into the trivial solution $f = 1$ when $J = 0$, and the minus sign gives an overdriven wave (shock wave when $J = 0$). The Chapman–Jouguet wave speed results when the radical in (2.1d) is set equal to zero. In the model adopted here, only overdriven or Chapman–Jouguet waves are physically acceptable, because heat is added in the absorption layer following the leading shock; in that case, the flow must remain subsonic with respect to the wave front. Unlike the ordinary blast wave, the present flow will have a density ratio f which

remains a function of the wave velocity and front location as $M_D \to \infty$. This feature makes boundary conditions rather difficult to apply in the present situation.

The hydrodynamic equations are those for time-dependent, compressible, inviscid, isentropic flow. r and θ are the spherical radius and polar angle, t is time and u_r and u_θ are the radial and tangential velocity components.

The laser radiation is characterized by its power distribution $\Pi(\theta, t)$. The heat flux J is then given by $J = \Pi/r_d^2$, where $r_d(\theta, t)$ is the wave-front radius. Self-similarity is obtained when the pressure p_0 in the undisturbed medium can be neglected and $\Pi(\theta, t)$ is of the form

$$\Pi(\theta, t) \equiv \Pi_L g(\theta), \tag{2.2}$$

where Π_L is constant (in fact, the requirement for self-similarity is less stringent: Π_L can be a power of time; the present analysis, however, has been limited to power constant in time) and $g(\theta)$ is an arbitrary function of the polar angle θ. The similarity variable λ is readily obtained from familiar dimensional arguments, or by requiring boundary conditions (2.1) to be time independent:

$$\lambda \equiv \frac{r}{At^n}, \quad \text{with} \quad n = \tfrac{3}{5}, \quad \text{and} \quad A \equiv \left[\frac{\Pi_L}{\rho_0}(\gamma - 1)a\right]^{\frac{1}{5}}. \tag{2.3}$$

a is a constant to be obtained as part of the solution in such a way that $\lambda = 1$ corresponds to the boundary of the spherically symmetric spark. Since no new length is introduced by the angular distribution $g(\theta)$ it is not surprising that the self-similar variables are similar to those for the purely spherical case of Champetier *et al.* and Wilson & Turcotte. If the wave front is defined as a function of θ,

$$\lambda_d \equiv h(\theta), \tag{2.4}$$

and physical variables are made non-dimensional as follows,

$$u_r(r, \theta, t) \equiv nAt^{n-1}V(\lambda, \theta), \quad u_\theta(r, \theta, t) \equiv nAt^{n-1}W(\lambda, \theta), \tag{2.5a, b}$$

$$\rho(r, \theta, t) \equiv \rho_0 R(\lambda, \theta), \quad p(r, \theta, t) \equiv \rho_0 (nAt^{n-1})^2 P(\lambda, \theta), \tag{2.5c, d}$$

then the flow equations read

$$LR + R\left(V_\lambda + 2\frac{V}{\lambda} + \frac{W_\theta}{\lambda} + \frac{W}{\lambda}\cot\theta\right) = 0, \tag{2.6a}$$

$$LV + \frac{n-1}{n}V - \frac{W^2}{\lambda} + \frac{P_\lambda}{R} = 0, \tag{2.6b}$$

$$LW + \frac{n-1}{n}W + \frac{VW}{\lambda} + \frac{P_\theta}{\lambda R} = 0, \tag{2.6c}$$

$$LP + 2\frac{n-1}{n}P + \gamma P\left(V_\lambda + 2\frac{V}{\lambda} + \frac{W_\theta}{\lambda} + \frac{W}{\lambda}\cot\theta\right) = 0, \tag{2.6d}$$

where L is the linear differential operator

$$L \equiv (V - \lambda)\frac{\partial}{\partial\lambda} + \frac{W}{\lambda}\frac{\partial}{\partial\theta}. \tag{2.7}$$

Boundary conditions (2.1) at $\lambda = h(\theta)$, expressed in self-similar form, appear as follows:

$$V_d = (1-f)h(1+h'^2/h^2)^{-1}, \tag{2.8a}$$

$$W_d = -(1-f)h'(1+h'^2/h^2)^{-1}, \tag{2.8b}$$

$$R_d = 1/f, \tag{2.8c}$$

$$P_d = (1-f)h^2(1+h'^2/h^2)^{-1}, \tag{2.8d}$$

$$f = \frac{1}{\gamma+1}\left\{\gamma - \left[1 - 2\frac{\gamma+1}{an^3}\frac{g(\theta)}{h(\theta)^5}\left(1+\frac{h'^2}{h^2}\right)\right]^{\frac{1}{2}}\right\}, \tag{2.8e}$$

where h' is the derivative of $h(\theta)$.

Given $g(\theta)$, the problem is now to solve the nonlinear system of partial differential equations (2.6) subject to boundary conditions (2.8) applied at a location $h(\theta)$ which is unknown *a priori*.

3. Small perturbation of a spherical detonation wave

A nearly spherical power distribution is considered, with ϵ representing the departure from spherical symmetry. The perturbation is developed in a series of Legendre polynomials $\mathscr{P}_k$ of argument $\cos\theta$:

$$g(\theta) \equiv \frac{1}{4\pi}\left[1 + \epsilon\sum_{k=1}^{\infty}\mathscr{P}_k(\cos\theta)\,A_k\right], \tag{3.1}$$

where the A_k are constants. Exclusion of the zeroth harmonic ensures that the total power is the same as for the purely spherical case.

The wave-front perturbation is assumed to have the same form, to first order in ϵ:

$$h(\theta) \equiv 1 + \epsilon\sum_{k=1}^{\infty}\mathscr{P}_k(\cos\theta)\,X_k, \tag{3.2}$$

where the X_k are unknown constants to be determined as part of the solution. Substituting (3.1) and (3.2) into (2.8*a–e*), the boundary conditions are expanded in series in integer powers of ϵ; this is possible because the zeroth-order (spherically symmetric) wave front is overdriven, and the radical in (2.8*e*) is therefore non-zero.

Consistency suggests similar expansions for the various physical variables throughout the flow field. To first order in ϵ,

$$V(\lambda,\theta) \equiv V^{(0)}(\lambda) + \epsilon\sum_{k=1}^{\infty}\mathscr{P}_k(\cos\theta)\,\hat{V}_k(\lambda), \tag{3.3a}$$

$$W(\lambda,\theta) \equiv \epsilon\sum_{k=1}^{\infty}\frac{d}{d\theta}\mathscr{P}_k(\cos\theta)\,\hat{W}_k(\lambda), \tag{3.3b}$$

$$R(\lambda,\theta) \equiv R^{(0)}(\lambda) + \epsilon\sum_{k=1}^{\infty}\mathscr{P}_k(\cos\theta)\,\hat{R}_k(\lambda), \tag{3.3c}$$

$$P(\lambda,\theta) \equiv P^{(0)}(\lambda) + \epsilon\sum_{k=1}^{\infty}\mathscr{P}_k(\cos\theta)\,\hat{P}_k(\lambda). \tag{3.3d}$$

Although the expansions are strictly correct at the boundary, there is no guarantee that they are uniformly valid for all values of λ; indeed, it will be shown that they become singular in the neighbourhood of $\lambda = 0$.

Zeroth-order solution

Collecting the $O(1)$ terms in the flow equations (2.6) and boundary conditions (2.8) gives

$$(V^{(0)}-\lambda)R^{(0)\prime}+R^{(0)}V^{(0)\prime}+2R^{(0)}V^{(0)}/\lambda=0, \tag{3.4a}$$

$$\frac{n-1}{n}V^{(0)}+(V^{(0)}-\lambda)V^{(0)\prime}+\frac{1}{R^{(0)}}P^{(0)\prime}=0, \tag{3.4b}$$

$$2\frac{n-1}{n}P^{(0)}+(V^{(0)}-\lambda)P^{(0)\prime}+\gamma P^{(0)}V^{(0)\prime}+2\gamma\frac{P^{(0)}V^{(0)}}{\lambda}=0, \tag{3.4c}$$

$$V^{(0)}(1)=1-f^{(0)}, \quad R^{(0)}(1)=1/f^{(0)}, \tag{3.5a,b}$$

$$P^{(0)}(1)=1-f^{(0)}, \tag{3.5c}$$

where a prime stands for $d/d\lambda$ and $f^{(0)}$ is defined as

$$f^{(0)}=\frac{1}{\gamma+1}\left[\gamma-\left(1-\frac{\gamma+1}{2\pi n^3 a}\right)^{\frac{1}{2}}\right], \tag{3.6}$$

in which a remains to be determined.

In effect, these equations have been integrated numerically by Wilson & Turcotte (1970). Their results were obtained by matching with the leading term of a Taylor series in λ, near the origin. The accuracy of this procedure proved insufficient for the present purpose; the solution must be more fully described near the origin if it is to serve as the basis for the calculation of first-order perturbations.

In order to recalculate the zeroth-order solution, we numerically integrate the system of differential equations (3.4) outwards from the origin towards the shock boundary. To move away from the origin, sufficiently detailed expansions in powers of λ are needed. With

$$\mu\equiv\lambda^{\alpha} \tag{3.7}$$

one finds

$$V^{(0)}=\lambda\sum_{j=0}^{\infty}a_j\mu^j, \quad R^{(0)}=\frac{1}{\lambda^2}\sum_{j=1}^{\infty}b_j\mu^j, \tag{3.8a,b}$$

$$P^{(0)}=\sum_{j=0}^{\infty}c_j\mu^j. \tag{3.8c}$$

For the particular value $\gamma=\frac{5}{3}$,

$$a_0=-\frac{2}{3\gamma}\frac{n-1}{n}=\frac{4}{15}, \tag{3.9}$$

$$\alpha\equiv-\frac{a_0+2}{a_0-1}=\frac{34}{11}. \tag{3.10}$$

α not being an integer makes all variables singular near $\lambda=0$ in the sense that derivatives of high enough order are always unbounded. As in classical blast-wave theory, the density goes to zero and the pressure remains bounded, and therefore the temperature is infinite at the focus. Expansions (3.8) turn out to contain only two free parameters, b_1 and c_0; other a_j, b_j and c_j were computed from b_1 and c_0 by George (1972). Since the unknown constant a appears in the three shock boundary conditions (3.5) their number is in effect reduced to two. Initial guesses are made for b_1 and c_0, equations (3.4) are integrated to the shock, and a standard linear correction scheme is used to modify the initial choices in

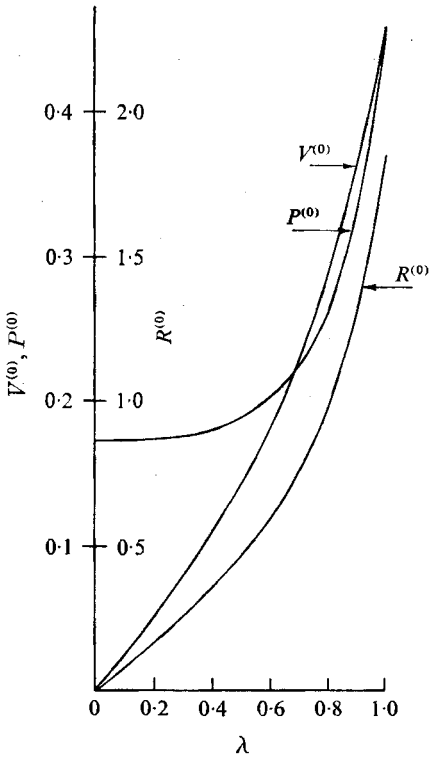

FIGURE 2. Velocity, density and pressure profiles of a spherically symmetric spark when $\gamma = \frac{5}{3}$.

order to satisfy the two boundary conditions; finally, a is computed. The results are

$$b_1 = 0{\cdot}9300, \quad c_0 = 0{\cdot}1731, \quad a = 1{\cdot}990. \tag{3.11}$$

The velocity, density and pressure profiles are plotted on figure 2 versus non-dimensional distance λ. Presented in this form, these results are in good agreement with those of Wilson & Turcotte (1970) except near the origin, where the present velocity is about 10 % lower than theirs.

A brief comparison can be made with constant-energy blast waves. In the present case, boundary conditions (3.5) explicitly contain the wave-front velocity. This simply reflects the difference in the mechanism which drives the leading shock wave: in a blast wave, the energy, initially released at the focus, is redistributed in the flow field, whereas in the present case, energy is deposited right behind the shock, pushing it forward.

The density profile, in particular, is much less steep near the boundary than that of a blast wave; indeed, when $\gamma = 1$ all profiles remain perfectly smooth, as shown by George (1972), and there is no Newtonian layer of concentrated mass near the shock. The reason, again, is that across an absorption layer the density ratio is not inversely proportional to $\gamma - 1$ and thus can remain finite when $\gamma \to 1$. From another point of view, particle trajectories do not become similarity lines in this case as they do in the blast wave; therefore mass is continuously flowing into the inner region of the plasma, which excludes the idea of a Newtonian layer.

On that basis, the 'locally radial' flow approximation as used, for instance, by Laumbach & Probstein (1969) in their study of blast waves in an exponential atmosphere is ruled out in the present case.

First-order solution

Collecting the $O(\epsilon)$ terms in (2.6) and (2.8) yields a linear system of differential equations and boundary conditions. Each harmonic is treated separately, the calculation being made for individual values $A_k = 1$. Linear superposition can then be used to derive the effect of any particular power perturbation.

For harmonic k, the flow equations read

$$R^{(0)}\hat{V}_k' + \left(R^{(0)\prime} + 2\frac{R^{(0)}}{\lambda}\right)\hat{V}_k - \frac{R^{(0)}}{\lambda}k(k+1)\hat{W}_k + (V^{(0)}-\lambda)\hat{R}_k' + \left(V^{(0)\prime} + 2\frac{V^{(0)}}{\lambda}\right)\hat{R}_k = 0, \tag{3.12a}$$

$$(V^{(0)}-\lambda)\hat{V}_k' + \left(\frac{n-1}{n} + V^{(0)\prime}\right)\hat{V}_k - \frac{P^{(0)\prime}}{R^{(0)2}}\hat{R}_k + \frac{1}{R^{(0)}}\hat{P}_k' = 0, \tag{3.12b}$$

$$(V^{(0)}-\lambda)\hat{W}_k' + \left(\frac{n-1}{n} + \frac{V^{(0)}}{\lambda}\right)\hat{W}_k + \frac{1}{R^{(0)}}\frac{1}{\lambda}\hat{P}_k = 0, \tag{3.12c}$$

$$\gamma P^{(0)}\hat{V}_k' + \left(P^{(0)\prime} + 2\gamma\frac{P^{(0)}}{\lambda}\right)\hat{V}_k - \frac{P^{(0)}}{\lambda}\gamma k(k+1)\hat{W}_k + (V^{(0)}-\lambda)\hat{P}_k' + \left(2\frac{n-1}{n} + \gamma V^{(0)\prime} + 2\gamma\frac{V^{(0)}}{\lambda}\right)\hat{P}_k = 0. \tag{3.12d}$$

The boundary conditions are transferred to the location $\lambda = 1$ by a Taylor expansion:

$$\hat{V}_k(1) = -K + [1 - f^{(0)} + 5K - V^{(0)\prime}(1)]\,X_k, \tag{3.13a}$$

$$\hat{W}_k(1) = -(1 - f^{(0)})\,X_k, \tag{3.13b}$$

$$\hat{R}_k(1) = -\frac{K}{f^{(0)2}} + \left[5\frac{K}{f^{(0)2}} - R^{(0)\prime}(1)\right]X_k, \tag{3.13c}$$

$$\hat{P}_k(1) = -K + [2(1 - f^{(0)}) + 5K - P^{(0)\prime}(1)]\,X_k, \tag{3.13d}$$

where K is the constant

$$K \equiv \frac{1}{4\pi n^3 a}\left(1 - \frac{\gamma+1}{2\pi n^3 a}\right)^{-\frac{1}{2}}. \tag{3.14}$$

The linear homogenous system (3.12) is integrated outwards from $\lambda = 0$ to $\lambda = 1$. Starting this numerical procedure requires expansions valid in the neighbourhood of the origin. Specializing (3.12) to small λ is done by retaining only the first term in the expansions of the coefficients which depend on the zeroth-order results (3.8). A solution is then sought of the form

$$\hat{V} \sim \lambda^m, \quad \hat{W} \sim \lambda^m, \quad \hat{R} \sim \lambda^{m+\alpha-3}, \quad \hat{P} \sim \lambda^{m+\alpha-1}. \tag{3.15}$$

An algebraic fourth-order indicial equation is obtained for m. The roots for the first ten harmonics are listed in table 1. A definite pattern emerges for increasing k: the first root m_k is positive and increasing; the pair of complex conjugate roots

Harmonic k	Roots m_k	$m_{rk} \pm i m_{ik}$	m'_k
1	1·114	$-0{\cdot}6253 \pm 0{\cdot}5500i$	−3·500
2	1·399	$-0{\cdot}2491 \pm 0{\cdot}7055i$	−4·537
3	1·941	$-0{\cdot}0137 \pm 0{\cdot}6691i$	−5·550
4	2·719	$0{\cdot}0998 \pm 0{\cdot}5965i$	−6·555
5	3·619	$0{\cdot}1510 \pm 0{\cdot}5413i$	−7·557
6	4·569	$0{\cdot}1767 \pm 0{\cdot}5047i$	−8·558
7	5·540	$0{\cdot}1912 \pm 0{\cdot}4802i$	−9·559
8	6·522	$0{\cdot}2002 \pm 0{\cdot}4632i$	−10·56
9	7·510	$0{\cdot}2061 \pm 0{\cdot}4511i$	−11·56
10	8·510	$0{\cdot}2103 \pm 0{\cdot}4421i$	−12·56

TABLE 1. Roots of the indicial equation corresponding to the focal singularity ($\gamma = \frac{5}{3}$)

$m_{rk} \pm i m_{ik}$ has an increasing real part, first negative, then positive, but always remaining less than 1; the fourth root m'_k is negative and decreasing.

The complete expansions possess four terms:

$$\hat{V}_k(\lambda) = A_{1k}\lambda^{m_k} + B_{1k}\lambda^{m_{rk}+im_{ik}} + B^*_{ik}\lambda^{m_{rk}-im_{ik}} + D_{1k}\lambda^{m'_k}, \tag{3.16a}$$

$$\hat{W}_k(\lambda) = A_{2k}\lambda^{m_k} + B_{2k}\lambda^{m_{rk}+im_{ik}} + B^*_{2k}\lambda^{m_{rk}-im_{ik}} + D_{2k}\lambda^{m'_k}, \tag{3.16b}$$

$$\hat{R}_k(\lambda) = \lambda^{\alpha-3}(A_{3k}\lambda^{m_k} + B_{3k}\lambda^{m_{rk}+im_{ik}} + B^*_{3k}\lambda^{m_{rk}-im_{ik}} + D_{3k}\lambda^{m'_k}), \tag{3.16c}$$

$$\hat{P}_k(\lambda) = \lambda^{\alpha-1}(A_{4k}\lambda^{m_k} + B_{4k}\lambda^{m_{rk}+im_{ik}} + B^*_{4k}\lambda^{m_{rk}-im_{ik}} + D_{4k}\lambda^{m'_k}), \tag{3.16d}$$

where * stands for 'complex conjugate'. The A's and D's are real constants, and the B's are complex constants. Note that the two middle terms in (3.16) combine into real oscillating functions of argument $m_{ik}\ln\lambda$. Four real constants are arbitrary, namely A_{1k}, $\mathrm{Re}\,(B_{1k})$, $\mathrm{Im}\,(B_{1k})$ and D_{1k}; all other constants are related to these (George 1972).

Boundary conditions (3.13) contain the unknown X_k, and therefore can be reduced to three given conditions. One solution of the linear fourth-order system of differential equations must therefore be dropped. D_{1k} and hence all the D's are set equal to zero on the physical grounds that the corresponding solution yields a source of mass, momentum and energy at the origin, for all harmonics.† Furthermore, the singularity corresponding to m'_k gets stronger for increasing k, which is incompatible with a more and more spherically symmetric geometry.

The system (3.12) is integrated using a fourth-order Runge–Kutta numerical scheme. Taking advantage of the principle of superposition of linearly independent solutions the three free constants A_{1k}, $\mathrm{Re}\,(B_{1k})$ and $\mathrm{Im}\,(B_{1k})$ are determined so as to satisfy boundary conditions.

The results describing the wave-front position and physical conditions behind it are presented in table 2 for individual harmonics 1–5. The magnitude of the shape perturbation is given by X_k (see (3.2)). All the X_k are positive, indicating that an increase in laser power creates an outward displacement of the wave front, and thus

† This is demonstrated in §4.

k	$\mathscr{P}_k(\nu)$ $(\nu \equiv \cos\theta)$	X_k	Z_{Vk}	$W_k(1)$	Z_{R_k}	Z_{Pk}
1	ν	0·1903	0·0491	0·0875	−0·1297	0·1366
2	$\frac{1}{2}(3\nu^2-1)$	0·1754	−0·0164	0·0806	−0·3325	0·0642
3	$\frac{1}{2}(5\nu^3-3\nu)$	0·1589	−0·0891	0·0730	−0·557	−0·0160
4	$\frac{1}{8}(34\nu^4-30\nu^2+3)$	0·1429	−0·1586	0·0656	−0·773	−0·0939
5	$\frac{1}{8}(63\nu^5-70\nu^3+15\nu)$	0·1288	−0·2217	0·0591	−0·965	−0·1625

TABLE 2. Spark shape and values of velocities, density and pressure behind the wave front, to first order in ϵ.

Power distribution: $g(\theta) = (4\pi)^{-1}[1+\epsilon\mathscr{P}_k(\cos\theta)]$.
Wave front: $h(\theta) = 1+\epsilon\mathscr{P}_k(\cos\theta)X_k$.
Radial velocity behind the wave: $V_d = 1-f^{(0)}+\epsilon\mathscr{P}_k(\cos\theta)Z_{Vk}$.
Tangential velocity behind the wave: $W_d = -\epsilon(d\mathscr{P}_k(\cos\theta)/d\theta)\,\hat{W}_k(1)$.
Density behind the wave: $R_d = 1/f^{(0)}+\epsilon\mathscr{P}_k(\cos\theta)Z_{Rk}$.
Pressure behind the wave: $P_d = 1-f^{(0)}+\epsilon\mathscr{P}_k(\cos\theta)Z_{Pk}$.

$$f^{(0)} = 0{\cdot}5404, \quad 1-f^{(0)} = 0{\cdot}4596, \quad 1/f^{(0)} = 1{\cdot}8504.$$

$$Z_{Vk} \boxminus V_k(1)+V^{(0)\prime}(1)X_k;$$

Z_{R_k} and Z_{Pk} are similarly related to $\hat{R}_k(1)$ and $\hat{P}_k(1)$.

an enhanced front velocity. The X_k decrease for increasing k, which shows that the shape perturbation is less for a more evenly distributed power perturbation.

The values of the radial velocity, tangential velocity, density and pressure behind the absorption front are also listed in table 2. The density perturbation at the front is negative in all cases, reflecting the fact that the influence of the shape perturbation dominates over that of the power perturbation. The absolute values of the radial velocity, density and pressure perturbations at the front increase with k; in fact, George has shown that they tend to asymptotic values for $k\to\infty$. As an indication, $\hat{V}_k(1)$ is displayed on figure 3(*b*) for $k = 1$ to $k = \infty$. The perturbation in tangential velocity decreases with k as it should for an increasingly spherically symmetric geometry.

The radial profiles of velocities, density and pressure perturbations are plotted on figures 3 (*a*)–(*d*) versus λ from $\lambda = 0$ to $\lambda = 1$. Note that $\lambda = 1$ is not exactly the physical boundary of the spark; the choice of λ was made (see (2.3)) so that the radial and tangential variables λ and θ remain independent of each other. The tangential velocity $\hat{W}_k$ must be negative at the wave front, because of the requirement that the velocity be normal to the front, and the properties of Legendre polynomials. Furthermore, $\hat{W}_k$ apparently remains negative over the whole range of λ. The density perturbation exhibits a change of sign from negative to positive at $\lambda = 0{\cdot}3$.

Although the character of the singularity near the origin changes between harmonics 3 and 4 (for example, the velocities become oscillatory but bounded for harmonics 4 and greater, whereas they are oscillatory and unbounded for the first three harmonics), no drastic change in the profiles appears to take place.

The limiting case of large wavenumber $k\to\infty$ is now examined. The original differential system (3.12) reduces from being fourth order to second order and the indicial equation describing the focal singularity yields only a pair of complex

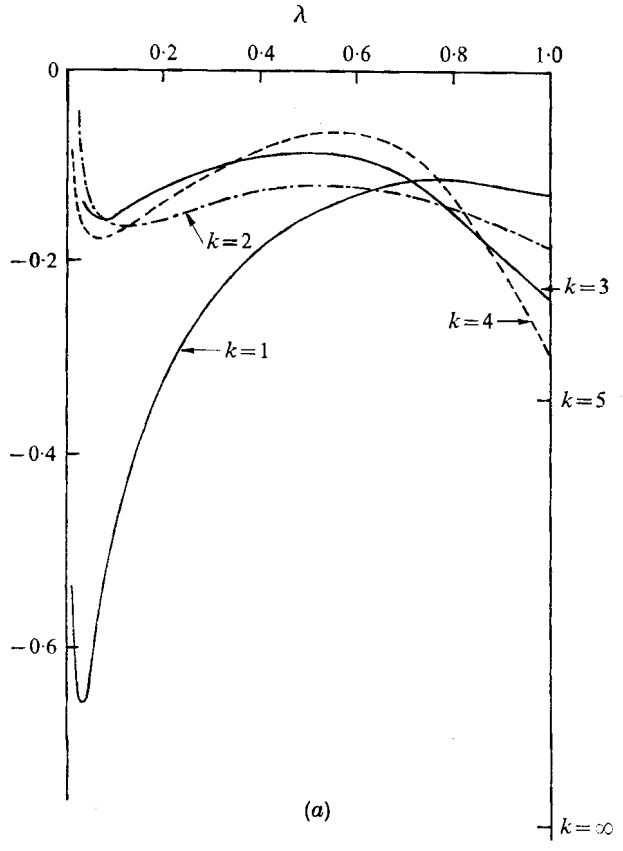

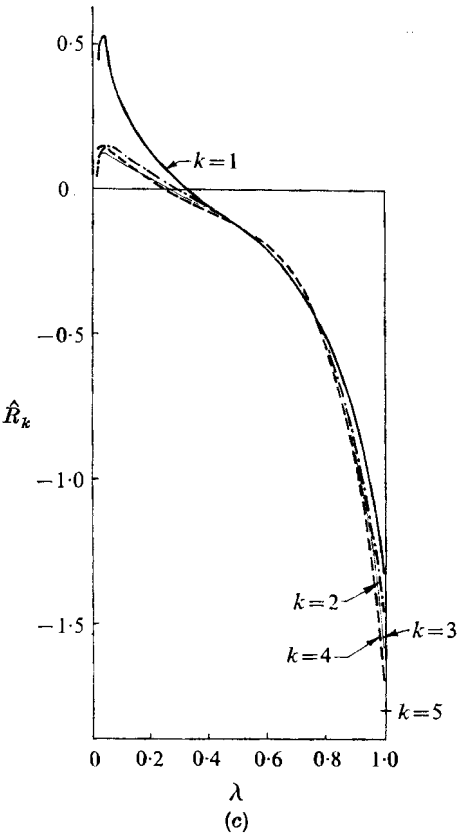

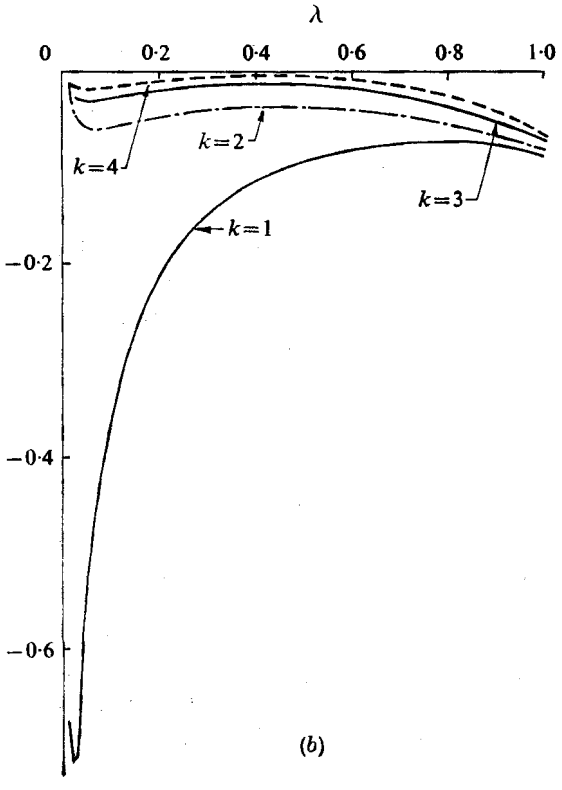

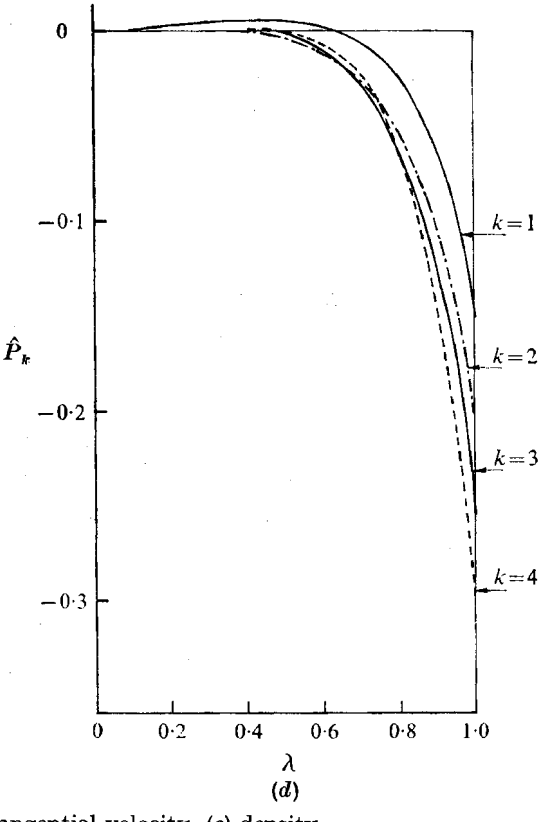

FIGURE 3. (*a*) Radial velocity, (*b*) tangential velocity, (*c*) density and (*d*) pressure perturbation profiles for harmonics 1–4.

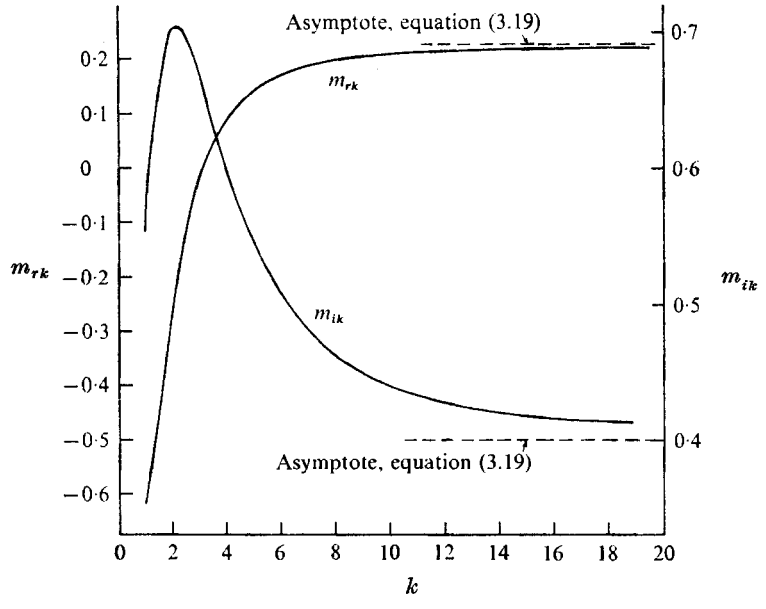

FIGURE 4. Complex conjugate roots of the indicial equation near the focus as a function of the harmonic number k.

conjugate roots. When $k \to \infty$, all quantities oscillate rapidly in the angular co-ordinate, giving rise to large θ derivatives:

$$d[\mathscr{P}_k(\cos\theta)]/d\theta \sim O(k) \quad \text{when} \quad k \to \infty. \tag{3.17}$$

The proper new ordering of physical variables is that $\hat{V}_k(\lambda)$ and $\hat{R}_k(\lambda)$ remain $O(1)$, whereas $\hat{W}_k(\lambda)$ and $\hat{P}_k(\lambda)$ become $O(1/k^2)$. Defining

$$\hat{W}_k(\lambda) \equiv k^{-2}\hat{\hat{W}}_k(\lambda), \quad \hat{P}_k(\lambda) \equiv \hat{\hat{P}}_k(\lambda) \tag{3.18a,b}$$

equation (3.12c) becomes $O(1/k^2)$ compared with (3.12a, b, d), which remain $O(1)$. It is easily seen that this system is only of second order. Specializing to the neighbourhood of the origin and looking for a solution of the type (3.15), a second-order algebraic equation is obtained, the roots of which are

$$m_{r\infty} \pm i m_{i\infty} = 0{\cdot}227 \pm 0{\cdot}400i. \tag{3.19}$$

The real and imaginary parts of the pair of complex conjugate roots of the complete fourth-order indicial equation are plotted on figure 4 for harmonics 1–20 as well as the asymptotic value for $k = \infty$ given by (3.19). The asymptotic values are quite closely approached for $k > 10$. It is seen that the real part m_{rk} always remains less than unity.

In the limit $k \to \infty$, the second-order system of differential equations cannot be expected to satisfy the three boundary conditions. Indeed, a boundary layer is called for in the neighbourhood of the wave front, of thickness $O(1/k)$. In that region, the proper ordering of physical variables, compatible with the boundary

conditions, is that $\hat{V}_k$, $\hat{R}_k$ and $\hat{P}_k$ are $O(1)$, but $\hat{W}_k$ and λ are to be transformed as follows:

$$\hat{W}_k \equiv k^{-1}\tilde{W}_k, \quad \lambda \equiv 1 - k^{-1}\tilde{\lambda}. \tag{3.20a,b}$$

Matching between the two regions appears feasible, but is not carried out in the present study.

4. Discussion of the flow singularity near the radiation focus

Although expansions (3.16) completely describe the singularity of the linear solution near $\lambda = 0$, a better understanding of the physical situation can be obtained by computing fluxes of mass, axial momentum and energy across a small sphere surrounding the focus. For example, consider the mass flux Q across a sphere of radius $\lambda_0 \ll 1$:

$$Q = 2\pi\rho_0 n A^3 t^{3n-1} \int_0^\pi RV\lambda_0^2 \sin\theta \, d\theta. \tag{4.1}$$

Expansions (3.3) are substituted into the integral, and use is made of the properties of Legendre polynomials. The $O(1)$ contribution is simply that of a spherically symmetric spark; there is no $O(\epsilon)$ contribution. In order to compute the $O(\epsilon^2)$ term, the corresponding differential equations have been solved for small λ by George (1972)

If the solution containing D's in (3.16) had been retained, the leading term in the $O(\epsilon^2)$ mass flux would have been

$$Q \sim \lambda_0^{2m'_k+\alpha-3}, \tag{4.2}$$

where k is the highest harmonic present. It is seen that, even for $k = 1$, the exponent of λ_0 is negative ($-5{\cdot}091$), thereby indicating a strong source of mass. Similar arguments can be used to show that a source of axial momentum $O(\epsilon)$ and a source of energy $O(\epsilon^2)$ are also implied. Therefore, because such sources are not contemplated in the present problem, the solutions containing D's should be rejected.

On the other hand, when the D's are set equal to zero, the leading term in the $O(\epsilon^2)$ flux has an amplitude

$$Q \sim \lambda_0^{2m_{rk}+\alpha-3}, \tag{4.3}$$

where k is the lowest harmonic present. The exponent is always positive, so that no source of mass exists in this case. The same is true for $O(\epsilon)$ axial momentum and $O(\epsilon^2)$ energy.

The remaining singularities of both A and B terms can be mathematically described in terms of singular perturbations. By inspection of the higher order systems of differential equations, an expansion of the mass flux in powers of ϵ can be obtained, say for the harmonic k

$$\begin{aligned} Q(\lambda_0) = c_0\lambda^{\alpha+1}[1 &+ \epsilon^2\lambda_0^{2(m_{rk}-1)}Q_2(\lambda_0) \\ &+ \epsilon^3\lambda_0^{3(m_{rk}-1)}Q_3(\lambda_0) + \epsilon^4\lambda_0^{4(m_{rk}-1)}Q_4(\lambda_0) + \ldots]. \end{aligned} \tag{4.4}$$

In this expression, Q_2, Q_3 and Q_4 are purely oscillating functions of λ_0 whose arguments are respectively $2m_{ik}\ln\lambda_0$, $3m_{ik}\ln\lambda_0$ and $4m_{ik}\ln\lambda$. Series (4.4) is uniformly convergent in Poincaré's sense outside a small focal region of size

$$\epsilon^{-1/(m_{r1}-1)} = \begin{cases} \epsilon^{0.615} & \text{for} \quad k = 1, \\ \epsilon^{1.29} & \text{for} \quad k = \infty. \end{cases} \tag{4.5}$$

Note that this region of non-uniformity exists for all harmonics since m_{rk} is always less than 1, and is larger for the smaller wavenumbers.

One must now ask whether the singular behaviour just described is due purely to linearization, or rather to neglected physical effects such as counter-pressure ahead of the shock or diffusion. We begin by considering the first possibility, and attempt to assess the importance of the nonlinear terms in the full inviscid equations (2.6) near the origin. For convenience, the dependent variables are slightly modified by extracting the leading part of the spherically symmetric solution:

$$V \equiv a_0\lambda + v, \quad W \equiv w, \tag{4.6a,b}$$

$$1/R \equiv \lambda^{-(\alpha-1)}(\lambda/b_1 + s), \tag{4.6c}$$

$$P \equiv c_0 + \lambda^{\alpha-1}(c_1\lambda + \hat{p}). \tag{4.6d}$$

The equations for v, w, s and $\hat{p}$ are listed in appendix A.

For illustrative purposes, a somewhat arbitrarily chosen model equation is discussed. Retaining only the linear and nonlinear radial velocity terms in the r-momentum equation (A 2) one gets

$$\Gamma\lambda v_{\lambda'} + v = vv_{\lambda'}, \tag{4.7}$$

where Γ and λ' are defined as

$$\Gamma \equiv (a_0 - 1)\left(a_0 + \frac{n-1}{n}\right)^{-1} = \tfrac{11}{6}, \quad \lambda' \equiv \left(a_0 + \frac{n-1}{n}\right)\lambda. \tag{4.8}$$

The model equation (4.7) is not 'correct' in any specific sense; rather, it is an illustrative combination of linear and nonlinear terms which appear in the full equations. We shall see that an understanding of the effect of the nonlinear term $vv_{\lambda'}$ in this equation will lead to a more systematic approach.

Equation (4.7) has a simple general solution which contains an arbitrary constant. This we choose in such a way that the part of the solution corresponding to the linear terms in (4.7) gives v to be of order ϵ. A direct comparison with the small perturbation solution is then possible. The solution reads

$$\lambda' = C\epsilon^{\Gamma}v^{-\Gamma} + (\Gamma+1)^{-1}v, \tag{4.9}$$

with C an arbitrary constant. The first two terms alone give the inverse-power relation $v \sim \lambda'^{-1/\Gamma}$, which corresponds to the linear perturbation solution already found for $\hat{V}_k$ (see (3.16)). The final term of (4.9) is due to the nonlinear right side of (4.7), and (with $C > 0$) has the effect of setting a minimum value of λ' below which there is no solution, namely

$$\lambda'_S = \epsilon^{\Gamma/(\Gamma+1)}\Gamma^{-\Gamma/(\Gamma+1)}[C(\Gamma+1)]^{1/(\Gamma+1)}. \tag{4.10}$$

Thus, including the nonlinear term in (4.7) reveals a 'forbidden zone' near $\lambda = 0$, which is of extent $\epsilon^{\Gamma/(\Gamma+1)} = \epsilon^{0.647}$, and into which the inviscid solution cannot be continued. In the linear approximation, this phenomenon is only indirectly represented, by a power-law singularity at the origin.

The foregoing ideas may be followed up more rigorously, as follows. In the large wavenumber limit, the ordering (3.18) is carried over to the full equations, considering that $w \sim O(1/k)$ and $\hat{p} \sim O(1/k^2)$; further, the system (A 1)–(A 4) is specialized to the polar axis of symmetry, on which θ derivatives of v and s vanish; finally, only the small λ region is of interest. Accordingly, (A 4) reduces to $\Phi = 0$ provided that v and w_θ lead over $\lambda^{\alpha+1}$, which may be verified *a posteriori*. Equations (A 1) and (A 2) then become decoupled and elimination of s provides the following nonlinear second-order equation:

$$\begin{aligned}(\alpha-2)\frac{\alpha c_1}{b_1}v+(a_0-1)^2\lambda^2 v_{\lambda\lambda}+(\alpha_0-1)\left(a_0+\frac{n-1}{n}\right)(\lambda v_\lambda - v)\\ +2(a_0-1)\lambda v v_{\lambda\lambda}+v^2 v_{\lambda\lambda}+(a_0-1)\lambda v_\lambda^2+v v_\lambda^2\\ +\left(3a_0+\frac{2n-1}{n}\right)v v_\lambda-(\alpha-1)\frac{1}{\lambda}v^2 v_\lambda-(\alpha-1)\left(a_0+\frac{n-1}{n}\right)\frac{v^2}{\lambda}=0. \quad (4.11)\end{aligned}$$

All nonlinear terms in (4.11) are of the same order in the region of non-uniformity of the small perturbation equations and thus must be retained.

We now ask if solutions of this more complicated, second-order equation also show a 'forbidden zone' as suggested by the model equation (4.7). Phase-plane methods are appropriate for this purpose, and we introduce the definitions

$$\xi \equiv \ln\lambda, \quad (4.12a)$$

$$v \equiv \lambda x_1(\xi), \quad dx_1/d\xi \equiv x_2(\xi). \quad (4.12b,c)$$

Equation (3.21) then becomes

$$\frac{dx_2}{dx_1} = \frac{-(x_1-N_1)x_2^2 - N_2(x_1-N_3)(x_1-N_1)x_2 + N_4 x_1(x_1-N_5)(x_1+a_0)}{x_2(x_1-N_1)^2}, \quad (4.13)$$

where the N's are numerical constants listed in appendix B. In principle, (4.13) should be integrated in the phase plane taking singularities into account; the physical location can then be obtained from (4.12*a*, *c*). However, sufficient information for our purpose is furnished by local solutions.

Equation (4.13) possesses five singular points: (0, 0), which is a focus (the corresponding solution for v reproduces the linear small perturbation solution (3.16) when $k = \infty$); $(N_5, 0)$, $(-a_0, 0)$ and (∞, ∞), which are saddle points; and the singularity $S(N_1, \infty)$. In the neighbourhood of S, (4.13) is readily integrated:

$$x_2 = C_1/(x_1 - N_1), \quad (4.14)$$

with C_1 an arbitrary constant. The corresponding solution for v is

$$(v - N_1\lambda)^2 = \lambda^2(C_2 \ln\lambda + C_3), \quad (4.15)$$

with C_2 and C_3 arbitrary constants. This result is interpreted as follows, with the aid of figure 5: singularity S is associated with points (v_S, λ_S) on the straight line $v = N_1\lambda$; the integral curves going through such a point behave, in its immediate neighbourhood, like

$$v - v_S = N_1(\lambda - \lambda_S) \pm [C_2\lambda_S(\lambda - \lambda_S)]^{\frac{1}{2}}. \quad (4.16)$$

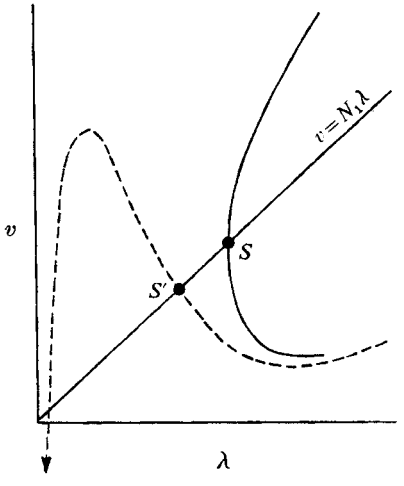

FIGURE 5. Sketch comparing singular first-order perturbation solution for radial velocity (dashed line) and the nonlinear solution (solid line) near the wave focus, for $k = \infty$.

They cross the line $v = N_1\lambda$ with an infinite slope, and furthermore, an integral curve coming from the region $\lambda > \lambda_S$ turns back towards that region. A forbidden domain this appears: $\lambda < \lambda_S$. The family of integral curves (4.16) has two parameters, namely the position λ_S at which the crossing occurs and the curvature of the square-root function (related to C_2). This allows matching with the small perturbation solution when $k \to \infty$, which also depends on two parameters. As a rough approximation to the size of the forbidden domain, the linear solution can be continued until it crosses the line $v = N_1\lambda$ at S'; one obtains $\lambda_{S'} = O(\epsilon^{1.291})$. This result is in agreement with the ordering arrived at by other perturbation considerations (see (4.5), for $k = \infty$).

Thus, the suggestion provided by the model equation (4.7) is confirmed. Of course, the existence of a forbidden domain has been established only on the axis of symmetry in the limit of large wavenumber, but this feature is thought likely to apply for all θ directions and wavenumbers, with a forbidden region all around the focus whose extent depends on wavenumber, perhaps being larger for smaller wavenumbers, as suggested by (4.5).

This situation is by no means exceptional for inviscid flows; a Prandtl–Meyer expansion flow around a corner of an angle larger than the critical angle also possesses a forbidden region. In the present case, the origin of this difficulty must be sought in the basic physical assumption made to derive the flow equations (2.6). Self-similarity requires neglecting the counter-pressure p_0 as well as neglecting viscosity and heat conduction. It may be shown† that infinite temperature at the focus of a spherically symmetric wave still prevails when the counter-pressure is introduced as a small perturbation in the boundary conditions. It is believed that the infinite temperature situation is responsible for the singularity in the asymmetric case. Indeed, each particle retains the entropy it got when it was first processed by the absorption layer, but there always exists

† A note to this effect is in preparation.

near the focus a region where particle velocities are very low. The fluid particles there have high entropies because they were processed at early times, but have different entropies according to the angle at which they crossed the front. Very strong angular gradients therefore exist near the focus; in a more refined physical model, these would be smoothed out by diffusion processes including radiative transfer. The present situation bears a certain analogy to the entropy singularity encountered in the so-called Ferri layer next to the surface of a cone in supersonic flow at an angle of attack (Ferri 1950).

5. Concluding remarks

A linear small perturbation scheme is apparently valid for the major part of this flow; in particular, the perturbed shape of the spark and changes in physical quantities behind the energy absorption layer are predicted for small asymmetry. Linear perturbations lead, however, to a singularity with a strong oscillating character in the neighbourhood of the focus; the lines of constant phase for all first-order variables are in fact logarithmic spirals around the origin. The meaning of this singularity has been elucidated by considering the full nonlinear flow equations. Analysis for the large wavenumber limit has revealed the existence of a forbidden domain which cannot properly be taken into consideration within the scope of the inviscid theory used here. A more refined model should include diffusion processes, such as electron conduction, which would tend to create a uniform, high temperature core. Then, of course, self-similarity would no longer be valid, and distinctions between early and late times would need to be made.

Some of the present conclusions can be directly applied to constant-energy blast waves developing into an atmosphere with an angular distribution of density; say, $\rho = \rho_0[1+\epsilon' G(\theta)]$. The singularity appearing in a linear small perturbation scheme is easily identified: with $n = \frac{2}{5}$ and $\gamma = \frac{5}{3}$ the expansions (3.8) remain valid, with $a_0 = \frac{3}{5}$ and $\alpha = \frac{13}{2}$. The roots of the indicial equation for the first-order singularity exponent m are, for the first harmonic,

$$m_1 = 1{\cdot}67, \quad m_{r1} + i m_{i1} = -2{\cdot}0 \pm 1{\cdot}96i, \quad m_1' = -6{\cdot}42.$$

The nonlinear theory still prevails and yields a forbidden region. Therefore a detailed investigation of the region around the origin seems to be needed in the case of non-spherical constant-energy blast waves.

This research was supported by N.A.S.A. under Grant NGL-33-010-042, monitored by Dr John C. Evvard, Lewis Research Center.

Appendix A. Nonlinear equations near the origin

Substitution of (4.6) into the flow equations (2.6) yields

$$\frac{\alpha-2}{b_1} v + \frac{w s_\theta}{\lambda} + (a_0-1)(\lambda s_\lambda - s) + v s_\lambda - (\alpha-1)\frac{vs}{\lambda} - \left(\frac{1}{b_1}+\frac{s}{\lambda}\right)\Phi = 0, \qquad \text{(A 1)}$$

$$(a_0-1)\lambda v_\lambda + \left(a_0 + \frac{n-1}{n}\right) v + \alpha c_1 s + [\lambda \hat{p}_\lambda + (\alpha-1)\hat{p}]\left(\frac{1}{b_1}+\frac{s}{\lambda}\right) + v v_\lambda + \frac{w v_\theta}{\lambda} - \frac{w^2}{\lambda} = 0, \qquad \text{(A 2)}$$

$$(a_0-1)\lambda w_\lambda+\left(a_0+\frac{n-1}{n}\right)w+\left(\frac{1}{b_1}+\frac{s}{\lambda}\right)\hat{p}_\theta+vw_\lambda+\frac{ww_\theta}{\lambda}+\frac{vw}{\lambda}=0, \quad \text{(A 3)}$$

$$(a_0-1)\alpha c_1\lambda+\gamma\left(c_0\frac{1}{\lambda^\alpha}+c_1+\frac{1}{\lambda}\hat{p}\right)\Phi+\alpha c_1 v + \left(\frac{v}{\lambda}+a_0-1\right)[\lambda\hat{p}_\lambda+(\alpha-1)\hat{p}]+\frac{w}{\lambda}\hat{p}_\theta=0, \quad \text{(A 4)}$$

where
$$\Phi\equiv\lambda v_\lambda+2v+w_\theta+\cot\theta w. \quad \text{(A 5)}$$

Appendix B. Constants of phase-plane trajectory near the origin

The numerical values of the various constant N's are

$$N_1=-(a_0-1)=0{\cdot}733, \quad N_2=4-\alpha=0{\cdot}909,$$

$$N_3=-\frac{2a_0-1/n}{4-\alpha}=1{\cdot}244,$$

$$N_4=\alpha-2=1{\cdot}091, \quad N_5=-(a_0-1/n)=1{\cdot}396.$$

REFERENCES

Alcock, A. J., Demichelis, C., Hamal, K. & Tozer, B. A. 1968 *Phys. Rev. Lett.* **20**, 1095.

Ambartsumyan, R. V., Basov, N. G., Boilo, V. A., Zuev, V. S., Krokhin, O. N., Kryukov, P. G., Senat-Skii, Yu. V. & Stoilov, Yu. Yu. 1965 *Sov. Phys. J.E.T.P.* **21**, 1061.

Canto, C., Reuss, J.-D. & Veyrie, P. 1968 *Comptes Rendus*, **267**, 878.

Champetier, J.-L., Couairon, M. & Vandenboomgaerde, Y. 1968 *Comptes Rendus*, **267**, 1133.

Daiber, J. W. & Thompson, H. M. 1967 *Phys Fluids*, **10**, 1162.

Damon, E. K. & Tomlinson, R. G. 1963 *Appl. Opt.* **2**, 546.

Demichelis, C. 1969 *I.E.E.E. J. Quantum Electronics*, **5**, 188.

Ferri, A. 1950 Supersonic flow around circular cones at angle of attack. *N.A.C.A. Tech. Note*, no. 2236.

George, Y. H. 1972 Nearly spherical constant power detonation waves driven by focused radiation. Ph.D. dissertation, Cornell University.

Key, M. H. 1969 *J. Phys.* B **2**, 544.

Laumbach, D. A. & Probstein, R. F. 1969 *J. Fluid Mech.* **35**, 53.

Meyerand, R. G. & Haught, A. F. 1963 *Phys. Rev. Lett.* **11**, 401.

Panarella, E. & Savic, P. 1968 *Can. J. Phys.* **46**, 183.

Raizer, Yu. P. 1965 *Sov. Phys. J.E.T.P.* **21**, 1009.

Ramsden, S. A. & Savic, P. 1964 *Nature*, **203**, 1217.

Wilson, C. R. & Turcotte, D. L. 1970 *J. Fluid Mech.* **43**, 399.